Available online at www.sciencedirect.com

ScienceDirect

Procedia Manufacturing 50 (2020) 236–240

Procedia MANUFACTURING

www.elsevier.com/locate/procedia

18th International Conference Metal Forming 2020

Hole-flanging of AA7075-O sheets: conventional process versus SPIF

Marcos Borrego, Domingo Morales-Palma*, José Andrés López-Fernández, Andrés J. Martínez-Donaire, Gabriel Centeno, Carpóforo Vallellano

Dpt. Mechanical Engineering and Manufacturing, Universidad de Sevilla, Camino de los Descubrimientos s/n, 41092 Sevilla, Spain

* Corresponding author. Tel.: +34954481355. *E-mail address:* dmpalma@us.es

Abstract

Recently, the research interest in hole-flanging for small and medium-sized batches has turned from conventional press-working to SPIF due to the advantages of incremental forming, such as flexibility and cost of tools. Both technologies have been studied separately using different approaches and, therefore, most studies cannot be easily compared. The aim of this work is to provide a better understanding of the deformation process and the material formability in hole-flanging by critically comparing both forming processes. To this end, a series of experimental tests by press-working and a SPIF process in a single stage, using forming tools with same profile radii, are analysed. The material is AA7075-O sheet of 1.6-mm thickness. The deformation process is analysed by measuring circumferential and meridional strains along the flange using Digital Image Correlation techniques. The process limits are evaluated by using the traditional Limiting Forming Ratio (*LFR*), which defines the maximum reachable diameter of the flange related to the initial pre-cut hole performed, as well as two additional parameters based on either the flange height or the average thickness reduction. Results conclude that the *LFR* is not an appropriate measurement of flangeability in processes other than conventional press-working and that SPIF is the preferred process to perform hole flanges with more flexibility in shape

Keywords: Hole-flanging; Single-point incremental forming; Formability; Flangeability; Limiting forming ratio

Nomenclature

PW	Press-working
SPIF	Single-point incremental forming
SPIF1	SPIF in a single stage
LFR	Limiting forming ratio
HER	Hole expansion ratio
FLD	Forming limit diagram
FFL	Fracture forming limit
FLC	Forming limit curve (for necking)

1. Introduction

Hole-flanging is a common forming operation, especially in automotive and aeronautics. It strengths the hole edge, improves its appearance and provides additional support when joining sheet parts. This operation is carried out by clamping the sheet blank with a pre-cut hole and deforming the material around the hole in a single punch stroke. This conventional press-working (PW) method needs of large batches to counterbalance the cost of tooling and equipment. Alternatively to PW, in SPIF minimum tooling and common CNC machines are employed due to the incremental nature of the process where low forces are required.

Hole-flanging by PW has a long history of use and therefore there is an extensive amount of studies in scientific literature addressing the feasibility of the process, in which the formability is measured using the concept of *LFR* (limiting forming ratio). This parameter defines the maximum *HER* (hole expansion ratio) attainable by the material as**:**

10.1016/j.promfg.2020.08.044

$$\boldsymbol{HER} = \frac{\boldsymbol{d_f}}{\boldsymbol{d_0}};\ \boldsymbol{LFR} \equiv \boldsymbol{HER_{max}} \equiv \left.\frac{\boldsymbol{d_f}}{\boldsymbol{d_0}}\right|_{\boldsymbol{max}} \quad (1)$$

where d_0 is the pre-cut hole diameter and d_f is the inner diameter of the produced hole-flanged part.

The paper by Paul [1] presents a recent review of the parameters that affects the formability of hole flanging by PW, focused on the effect of punch geometry, the fundamentals of deformation and damage and the influence of uniaxial tensile properties among others factors. In particular, the works by Huang and Chien [2, 3] described the independency of the *LFR* in terms of punch radius as far as the failure at the edge of flanged hole is controlled by tensile stress in circumferential direction. Same conclusions have been observed in a recent experimental work by Borrego et al. [4], who also elucidated the actual influence of the bending effect induced by the punch edge radius. Despite the number of variables affecting the formability of PW operations, *LFR* has proven to be a valid measure of flangeability in PW.

On the other hand, SPIF has been the subject of numerous studies due to its flexibility and the apparent enhancement of the sheet formability, among other beneficial features compared with conventional sheet metal forming processes. Thus, there are relevant scientific works addressing the influence of material properties, material thickness, tool size, spindle speed, feed rate, step down, lubrication, tool path strategy, etc. The paper by Behera et al. [5] describes exhaustively the state of the art of this technology up to 2015, highlighting other main contributions in academia and industry.

The pioneering research on hole-flanging by SPIF belongs to Cui and Gao [6] who firstly analysed the formability of the process in terms of the *LFR* and thickness distribution using three different multi-stage strategies. Later, Centeno et al. [7] studied the influence of a pre-cut hole in the formability of SPIF and concluded that small pre-cut holes do not have any influence on the formability of the process if the plastic deformation does not reach the vicinity of the hole edge. However, in the opposite case, a new mode of failure is triggered that entails a combination of in-plane stretching in the flange and local bending induced by the forming tool, which causes a suppression of necking prior to fracture.

Due to the particular geometry of the holes, and probably inherited from the PW process, most studies on hole-flanging by SPIF have analysed the sheet formability via the *LFR*, and just a few authors, conscious about the limitations of *LFR*, have applied the Forming Limit Diagram (FLD) as an analysis tool. Among these authors, Centeno et al. [7] attained to explain the enhancement of formability in terms of necking suppression, as described above, analysing the strain distribution along the flange in the FLD. Silva et al. [8] justified the differences in *LFR* values of specimens by PW and multi-stage SPIF by analysing the strain paths in the FLD and their distances to the FLC (Forming Limit Curve for necking) and FFL (Fracture Forming Limit) curves. Montanari et al. [9] found an explanation to the different failure mechanisms of hole-flanging by PW and multi-stage SPIF based in the absence of changes in strain and stress paths at the transition from the FLC towards the FFL. Cristino et al. [10] analysed the strain paths of hole-flanging by SPIF to evaluate a new methodology for the determination of the experimental values of critical ductile damage and fracture toughness.

Recently, Borrego et al. [11] studied the hole-flanging process by a single-stage SPIF and analysed the enhancement of formability of the SPIF process and failure modes in the major-minor strain space compared to *LFR*, proposing others formability parameters alternative to this last one. The SPIF1 process reduces considerably the production time compared to multi-stage strategies and can provide functional flanges in practice assuming some geometrical restrictions. A step forward, to balance fabrication time and thickness distribution along the produced flange, is to perform a two-stage SPIF process optimizing the flange geometry in the first pass, as proposed by Morales-Palma et al. [12].

The aim of this work is to contribute to the comprehension of the factors that control the sheet formability in hole-flanging using two very different technologies: PW and SPIF1. To this end, experimental results of hole-flanging tests by both technologies using aluminium alloy 7075-O sheets of thickness 1.6 mm are analysed and compared. The formability of the flange is analysed via the traditional *LFR* and two parameters proposed by the authors in earlier publication, as well as the conventional FLC (for necking) and FFL (for fracture). The thickness profile of the flange is also discussed.

2. Experimental procedure

To perform the comparison between the two hole-flanging manufacturing technologies, an aluminium alloy 7075-O of 1.6-mm thickness was selected. The manufactured parts by PW and SPIF1 shared the same geometrical characteristics such as the initial and final hole diameters as well as tool radii of $R = 8$ mm in order to induce similar bending conditions in the flange during its deformation, where R is the edge radius of the punch in the PW process and the tool radius in SPIF1. This section presents the main results of the experimental hole-flanging tests.

2.1. Hole-flanging processes

An experimental campaign was planned to evaluate the hole-flanging formability limits by PW and SPIF1. Fig. 1 presents a schema of both hole-flanging processes as well as two of the specimens manufactured. The tests by PW were carried out using an Erichsen 142–20 machine with a blank holder and a 100-mm diameter die (see Fig. 1(a)). A punch with circumferential diameter $d_f = 95.8$ mm and edge radius $R = 8$ mm was used. The SPIF1 tests were carried out on an EMCO VMC-200 3-axis milling CNC machine. The SPIF setup comprised a blank holder and a backing plate with a 100-mm diameter hole (see Fig. 1(b)). The sheet blanks were fixed by the holder over the backing plate and were incrementally deformed by a hemispherical tool of radius $R = 8$ mm following a helical trajectory previously modeled and simulated in CATIA® using the machining workbench. The tool movement was set to 0.2 mm/turn of step down, 1000 mm/min of feed rate and 0 rpm (locked tool).

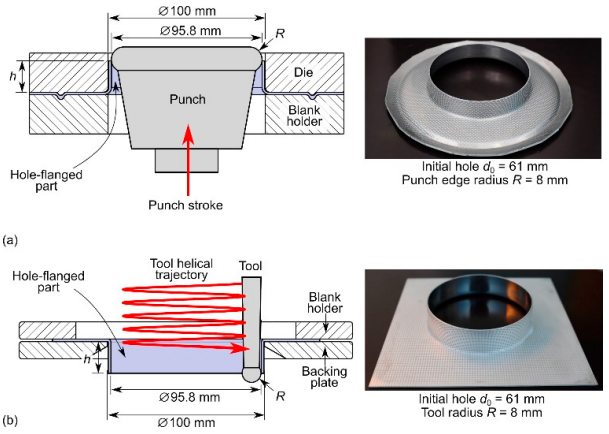

Fig. 1. Schema of hole-flanging processes and parts manufactured by (a) PW and (b) SPIF1.

The strains at the outer sheet surface were measured at the end of the test or after the specimens reached failure using the optical 3D strain analysis system ARGUS®. The strains at the hole edge, where ARGUS is not able to provide information, were calculated from direct measurement of the final and initial perimeter of the hole and the final and initial sheet thickness, and assuming material volume constancy. To analyze the geometric capability of the process, finished flanges were cut to measure the final height and the sheet thickness distribution along the flange.

Table 1. Successful (O), necked (N) and fractured (F) experimental hole-flanging tests by PW and SPIF1.

Initial pre-cut hole diameter, d_0	PW	SPIF1
57.0		F
58.0	N	
60.0	N	F
61.0	O	O
62.5		O
65.0	O	O

Table 1 presents the results of experimental tests. The successful and failed flanges by necking or ductile fracture are distinguished with O, N and F, respectively. The sheet blanks were cut out from the supplied sheets with circular holes of different diameters (d_0, see Table 1). The central holes were milled and subsequently ground with fine grit sandpaper to eliminate any burrs. For each type of experimental test, the hole diameter d_0 was adjusted in successive tests to identify the *LFR* value according to Eq. (1).

A representative specimen geometry, d_0 = 61 mm, is selected in this work to compare the results of both manufacturing technologies. These specimens are good candidates due to they were successfully tested in both hole-flanging operations and specimens with smaller holes failed by necking or by ductile fracture, as can be seen in Table 1.

3. Results

3.1. Strain analysis

The analysis of strain distribution allows understanding the geometrical differences of flanges manufactured by PW and SPIF1. In this regard, such differences in the strain space can be better understood by plotting the circumferential (ε_c) and meridional (ε_m) strains of the specimen instead of the traditional in-plane major and minor strains.

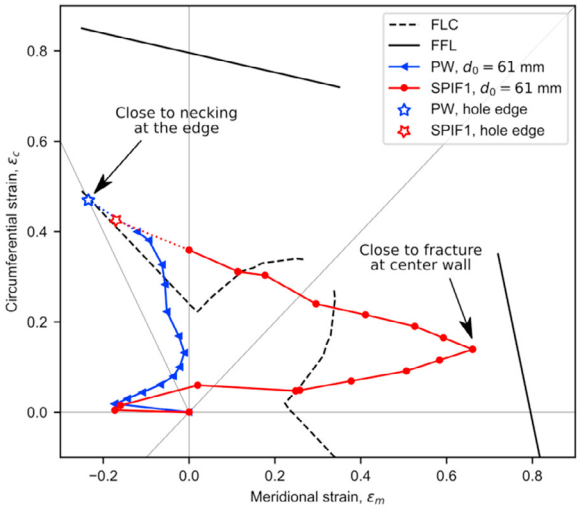

Fig. 2. Strain distribution by PW and SPIF1.

Fig. 2 presents the circumferential (ε_c) and meridional (ε_m) strain distribution at the outer sheet surface in flanged parts by PW and SPIF1 with d_0 = 61 mm. The measurements were performed along the flange following a path in the rolling direction. The solid lines represent strains measured with ARGUS®. Points represented with a star at the end of the dotted lines were obtained from direct measurements of thickness (to evaluate the thickness strain, ε_t) and circumferential perimeter in the hole edge (to evaluate ε_c, and estimating ε_m via volume constancy, as described above).

The strain distributions show that the SPIF1 process produces a flange with a central zone very stretched in the meridional direction (ε_m = 0.67) whereas, on the other hand, the specimen obtained by PW exhibits a slightly shortened flange along this direction ($\varepsilon_m < 0$).

Fig. 2 also shows that maximum circumferential strains for both SPIF1 and PW forming processes are about ε_c = 0.44 and 0.47, respectively, at the hole edge. Actually, a similar circumferential strain distribution was expected for both specimens due to the hole expansion process and such differences were attributed to the different d_f considered at the end of both processes. A value of final hole diameter equals to the punch diameter, d_f = 95.8 mm, was used for the PW process since the punch passed completely through the hole. However, despite the tool trajectory in SPIF1 was modeled to obtain a hole of d_f = 95.8 mm, the measured value of the final diameter was slightly lower (d_f = 94.8 mm) due to tool deflection and spring-back effects. Notice that, in theory, the distribution of ε_c along the final flange is not dependent of the forming process

can be determined from the change of the circumference length at every diameter $d \in [d_0, d_f]$. Thus, the circumferential strain is given by $\varepsilon_c = \ln(d/d_f)$ at the inner flange surface and $\varepsilon_c = \ln(d/(d_f + t))$ at the outer surface, where t is the flange thickness.

From a geometrical point of view, according to the strain distributions shown in Fig. 2, it is expected to obtain longer flanges by SPIF1 than by PW, but with less homogeneous thickness distribution along them.

The FLC for necking and FFL for fracture are also depicted in Fig. 2. Failed specimens, those with initial pre-cut diameter d_0 of 60 mm or less (see Table 1), failed by necking at the hole edge in PW tests and by fracture due to excessive thinning in the middle of the wall in SPIF1 tests, as reported in [4] and [11], respectively. As can be observed in Fig. 2 for the successful PW test, the strain at the hole edge is very close to the FLC, which indicates that necking was about to occur in that location. Likewise, for the successful SPIF1 test, the strain at the center wall above the FLC and close to the FFL indicates that the specimen was about to fracture without prior necking.

It should be noted that the strains near the hole edge in PW are clearly above the FLC (see Fig. 2). In a recent paper [4], authors showed that this apparent enhancement of formability can be attributed to the bending effect induced by the punch profile, and concluded that the conventional FLC is a suitable tool to analyse formability in hole-flanging only at the hole edge.

3.2. Formability measures

Table 2 summarizes the formability limits for PW and SPIF1. Several parameters are shown such as the minimum pre-cut hole diameter ($d_{0,min}$) attained without failure, the conventional *LFR*, the non-dimensional flange height (h/d_f) and the thickness ratio ($\bar{t}/t_0$). This last parameter was introduced by the authors in [4], where $\bar{t}$ is the average thickness obtained by assuming volume constancy during the flange deformation:

$$\frac{\pi}{4}\left({d_f}^2 - {d_0}^2\right)t_0 = \pi\left(d_f + \frac{\bar{t}}{2}\right)h\bar{t} \qquad (2)$$

Table 2. Formability measures in hole-flanging by PW and SPIF1.

	PW	SPIF1
Minimum initial hole diameter, $d_{0,min}$ (mm)	61.0	61.0
Limit forming ratio, *LFR*	1.57	1.55
Non-dimensional flange height, h/d_f	0.19	0.26
Thickness ratio, $\bar{t}/t_0$	0.78	0.56

As can be seen in Table 2, the *LFR* varies slightly (1.55 for PW and 1.57 for SPIF1) although the minimum pre-cut hole diameter in both processes was the same (d_0 = 61 mm). Indeed, for the calculation of the *LFR* according to Eq. (1), different values of final hole diameter were used, as described above. Notice that the *LFR* and the circumferential strain at the hole edge are closely related.

Taking into account that the *LFR* is almost the same in both processes although their formation processes are completely different, two complementary parameters to the *LFR* have been used to better evaluate flangeability: the non-dimensional flange height (h/d_f) and the thickness ratio ($\bar{t}/t_0$). The former is a measure of the material stretching in the meridional direction of the flange. The latter can be used to measure the average reduction in flange thickness as $1 - \bar{t}/t_0$. Therefore, the higher the flange height or the lower the flange thickness, the higher the formability. According to the data in Table 2, SPIF1 improves the flangeability by 37% of flange height and 100% of thickness reduction compared to PW.

3.3. Thickness distribution analysis

Fig. 3 shows the thickness distribution profiles corresponding to the selected successful hole-flanged parts obtained by PW and SPIF1 once specimens were cut along the flange. In agreement with the analysis in section 3.1, it is observed that the SPIF1 process produces a pronounced wavy thickness distribution along the flange with a maximum reduction of 50% around the middle of the flange. Instead, the flange by PW presents a more constant thickness reduction with the length as well as a lower height.

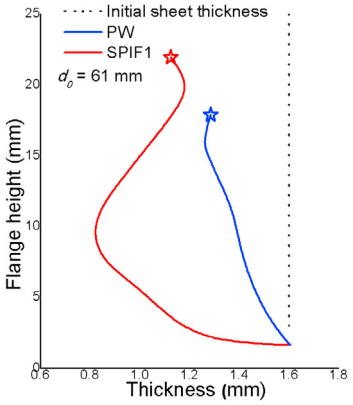

Fig. 3. Thickness distributions along the flange by PW and SPIF1.

As a result of the local and incremental deformation induced in the material by SPIF1, the material is intensively stretched in the meridional direction and, therefore, higher and thinner flanges are produced. Conversely, the conventional hole-flanging process provides shorter but thicker and more robust flanges. The practical application and service requirements of the flange would determine the more suitable process. The excessive thinning of the flange by SPIF1 may be improved using a multi-stage SPIF strategy [13]. However, multi-stage strategies have the disadvantage of increasing the production time as well as the process complexity. In this sense, the minimization of the number of stages and the optimisation of the intermediate shape between passes are mandatory to make the SPIF process competitive in practice [12].

4. Conclusions

Hole-flanging processes by PW and SPIF1 have been critically compared in terms of flangeability and flange

geometry. The main conclusions can be summarized as follows:

- Regarding the strain distribution along the flange, the main difference between both processes resides in the evolution of the meridional strain. In SPIF1, this strain displays a high positive value around the middle of the flange, which is responsible for a longer and thinner flange than the one in the conventional process for a given *HER* value.
- The traditional *LFR* does not allow evaluating the formability in hole-flanging by SPIF since it does not capture the physics of failure of this process. A *LFR* value of approximately 1.6 is obtained for both processes.
- The non-dimensional flange height (h/d_f) and thickness ratio ($\bar{t}/t_0$) are suitable parameters for evaluating flangeability in both processes. In terms of these parameters, SPIF1 exhibits a significant enhancement in flangeability regarding the PW process: up to 37% of flange height and 100% of average thickness reduction.

Acknowledgements

The authors wish to thank the Spanish Government (grants DPI2015-64047-R and PGC2018-095508-B-I00) and the Regional Government of Andalusia (grant US-1263138) for their financial support.

References

[1] Paul SK.. A critical review on hole expansion ratio. Materialia 2020;9:100566. doi:10.1016/j.mtla.2019.100566.

[2] Huang YM, Chien KH. Influence of the punch profile on the limitation of formability in the hole-flanging process. J Mater Process Tech 2001;113:720–4. doi:10.1016/S0924-0136(01)00597-0.

[3] Huang YM, Chien KH. The formability limitation of the hole-flanging process. J Mater Process Tech 2001;117:43–51. doi:10.1016/S0924-0136(01)01060-3.

[4] Borrego M, Morales-Palma D, Martínez-Donaire AJ, Centeno G, Vallellano C. Analysis of formability in conventional hole flanging of AA7075-O sheets: punch edge radius effect and limitations of the FLC. International Journal of Material Forming 2019. doi:10.1007/s12289-019-01487-2.

[5] Behera AK, de Sousa RA, Ingarao G, Oleksik V. Single point incremental forming: An assessment of the progress and technology trends from 2005 to 2015. J Manu Process 2017;27:37–62. doi:10.1016/j.jmapro.2017.03.014.

[6] Cui Z, Gao L. Studies on hole-flanging process using multistage incremental forming. CIRP J Manu Sci Tech 2010;2:124–8. doi:10.1016/J.CIRPJ.2010.02.001.

[7] Centeno G, Silva M, Cristino V, Vallellano C, Martins P. Hole-flanging by incremental sheet forming. Int J Mach Tool Manu 2012;59:46–54. doi:10.1016/j.ijmachtools.2012.03.007.

[8] Silva M, Teixeira P, Reis A, Martins P. On the formability of hole-flanging by incremental sheet forming. Proceedings of the Institution of Mechanical Engineers, Part L: Journal of Materials: Design and Applications 2013;227:91–9. doi:10.1177/1464420712474210.

[9] Montanari L, Cristino V, Silva M, Martins P. On the relative performance of hole-flanging by incremental sheet forming and conventional press-working. Proceedings of the Institution of Mechanical Engineers, Part L: Journal of Materials: Design and Applications 2014;228:312–22.doi:10.1177/1464420713492149.

[10] Cristino V, Montanari L, Silva M, Atkins A, Martins P. Fracture in hole-flanging produced by single point incremental forming. International J Mech Sci 2014;83:146–54. doi:10.1016/j.ijmecsci.2014.04.001.

[11] Borrego M, Morales-Palma D, Martnez-Donaire A, Centeno G, Vallellano C. Experimental study of hole-flanging by single-stage incremental sheet forming. J Mater Process Tech 2016;237:320–30. doi:10.1016/j.jmatprotec.2016.06.026.

[12] Morales-Palma D, Borrego M, Martínez-Donaire A, Centeno G, Vallellano C. Optimization of hole-flanging by single point incremental forming in two stages. Materials 2018;11:2029. doi:10.3390/ma11102029.

[13] Skjoedt M, Bay N, Endelt B, Ingarao G. Multi Stage Strategies for Single Point Incremental Forming of a Cup. Int J Mater Forming 2008;1:1199–202. doi:10.1007/s12289-008-0156-3.